nature materials

SUPPLEMENTARY INFORMATION

DOI: 10.1038/NMAT3072

Bifurcation-based acoustic switching and rectification

N. Boechler, G. Theocharis, and C. Daraio

Engineering and Applied Science, California Institute of Technology, Pasadena, CA 91125, USA

Supplementary information

Experimental configuration. The sensors are placed four sites from the actuator and at the end of the crystal. The sensor located four sites away from the actuator is used to measure the localized vibrations within the vicinity of the defect (without being in direct contact with it, so as to avoid affecting its dynamics). The sensor at the end of the crystal is used to measure the transmission through the crystal. For our rectifier geometry, the bifurcation-based rectification mechanism is only clearly evident with a defect placed two particles away from the actuator. For defect particles placed three or more particles away from the actuator, the high attenuation of the signal (with frequency within the band gap[1]) does not allow sufficient energy from the actuator to arrive to the defect particle. For defect particles placed next to the actuator, we observe that the effect of the boundary is dominant, and the dynamics of the system becomes more chaotic. The chain length of 19 particles was selected as a balance between having high enough attenuation (arising from the band gap) to demonstrate the rectification effect, and having a small enough dissipation of the signal to maximize the experimental tractability. In our numerical simulations, we observe that decreasing the dissipation in the system can increase the transmission efficiency in the forward configuration.

DOI: 10.1038/NMAT3072

Experimental measurement of linear spectra. To measure the linear spectrum of the system, we apply broadband noise via the actuator to the granular crystal[2,3] statically compressed at F_0 = 8 N. We calculate the transfer functions, shown in Fig. S1, by dividing the averaged (over 16 runs) PSD of the force-time history measured at each sensor, by the mean (over all runs) PSD amplitude in the acoustic band (1 kHz to f_c). In the reverse configuration (Fig. S1a), frequencies above the acoustic cutoff are attenuated. Alternatively, in the forward configuration (Fig. S1b) the actuator is placed close to the defect and excites the defect mode, as can be seen in the spectrum of the sensor two sites from the defect (blue curve). The localized nature of this mode is revealed, as this peak is not present at the end of the chain (red curve). The frequency peak observed here agrees closely with the analytically predicted defect mode frequency f_d (vertical dashed line).

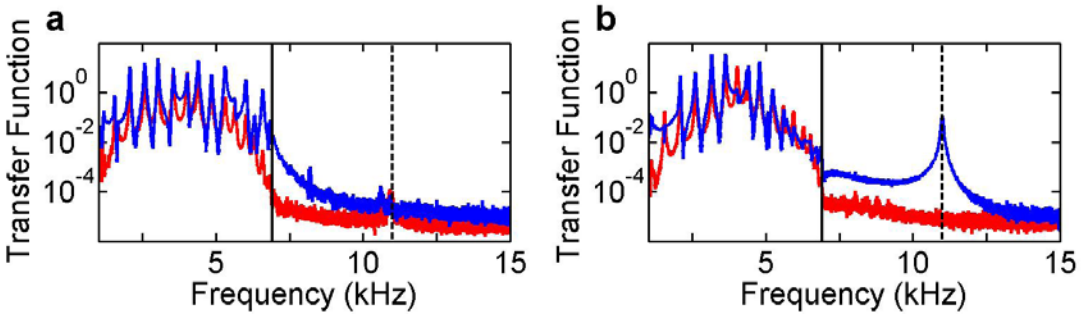

Figure S1. Experimentally measured PSD transfer functions. PSD transfer function for the granular crystal rectifiers of Figs. 1-4 (F_0 = 8 N) in the (a) reverse and (b) forward configurations. Blue (dark grey) curve is the sensor located four particles from the actuator, red (light grey) is the sensor 19 particles from the actuator (corresponding to the sensors of the same color in Fig. 1a,b, respectively). The vertical black line is the acoustic band upper cutoff frequency f_c, and the vertical black dashed line is the defect mode frequency f_d.

Quasiperiodic vibrations. To understand the fundamental mechanism that leads to quasiperiodic vibrations, we apply the Newton's method in phase space[2] to Eq. 1. This method is utilized for obtaining periodic solutions and their Floquet multipliers λ_j, which can be used to study the linear stability of the solutions. If all $|\lambda_j| < 1$, the periodic solution is stable as small perturbations decay exponentially in time. In Fig. S2a, we show the Floquet spectrum of the periodic solution corresponding to the forward configuration with $F_0 = 8$ N, $\tau = 1.75$ ms, $f_{dr} = 10.5$ kHz, and $\delta_{(+)} = 0.6$ μm. Here all Floquet multipliers lie on a circle of radius $e^{\frac{-1}{2\pi f_{dr}}}$ except four—two which lie outside the unit circle. Because of these two, the periodic solution corresponding to these parameters is linearly unstable. From a bifurcation point of view, this picture is known as a Naimark-Sacker bifurcation[4]. In this case, the unstable periodic solution decays into a stable two-frequency quasiperiodic solution. In Fig. S2b, we show the time evolution (force-time history of the fourth particle) of the unstable periodic solution of Fig. S2a. We numerically integrate the equations of motion (Eq.1) using a fourth-order Runge-Kutta scheme with the unstable periodic solution found by Newton's method as the initial condition. After a short transient period, we see the unstable periodic solution decays into a stable quasiperiodic solution. Multiple frequency peaks based on the linear combinations of two dominant frequencies (f_{dr} and f_N), characteristic of a quasiperiodic solution, can be seen in the PSD (calculated for times $100 < t < 200$ ms, blue region) shown in Fig. S2c, where the frequency peaks corresponding to higher order linear combinations have lower amplitude[5]. Similarly, to obtain the quasiperiodic branch of solutions of Fig. 2, we calculate the dynamic force amplitude by using the unstable periodic solution of the same

DOI: 10.1038/NMAT3072

driving amplitude as an initial condition for the numerical integrator. Here we integrate for 50 ms and take the maximum amplitude from 40-50 ms.

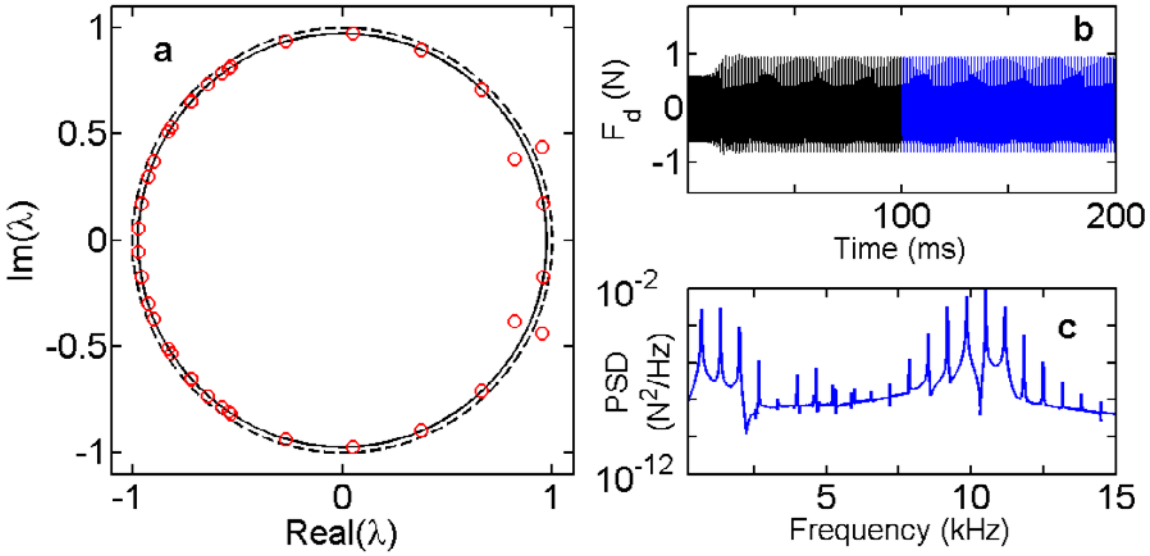

Figure S2. Quasiperiodic vibrations. (a) Floquet spectrum of the periodic solution corresponding to f_{dr}=10.5 kHz and $\delta_{(+)}$= 0.6 μm. **(b)** Numerically calculated force-time history of the fourth particle away from the actuator in the forward configuration, using as an initial condition the periodic solution of panel **(a)**. **(c)** PSD of the blue (dark grey) time region of panel **(b)**.

Route to chaos. In this section, we study the transition of the system from quasiperiodic to chaotic dynamics. Using the same method as described for Fig. S2, we take the PSD of the force-time history (four particles from the actuator) of the time integrated solution using the unstable periodic solutions found by Newton's method, at increasing amplitudes, as the initial conditions. For the smallest amplitude $\delta_{(+)}$= 0.60 μm we observe a quasiperiodic solution (Fig. S3a) with a discrete set of frequencies based on the linear combinations of f_{dr} and f_N. As we increase the amplitude ($\delta_{(+)}$= 1.0 μm, Fig. S3b), we

observe the appearance of additional peaks at frequencies based on linear combinations of $f_{dr}/2$ and $f_N/2$, which is a sign of double period bifurcation. Increasing the amplitude further ($\delta_{(+)} = 1.03$ μm, Fig. S3c) we see peaks based on $f_{dr}/4$ and $f_N/4$ (second double period bifurcation). Further increasing the amplitude, a continued cascade of double period bifurcations results in the merging of distinct frequency peaks and the formation of continuous bands, as shown in Fig. S3d.

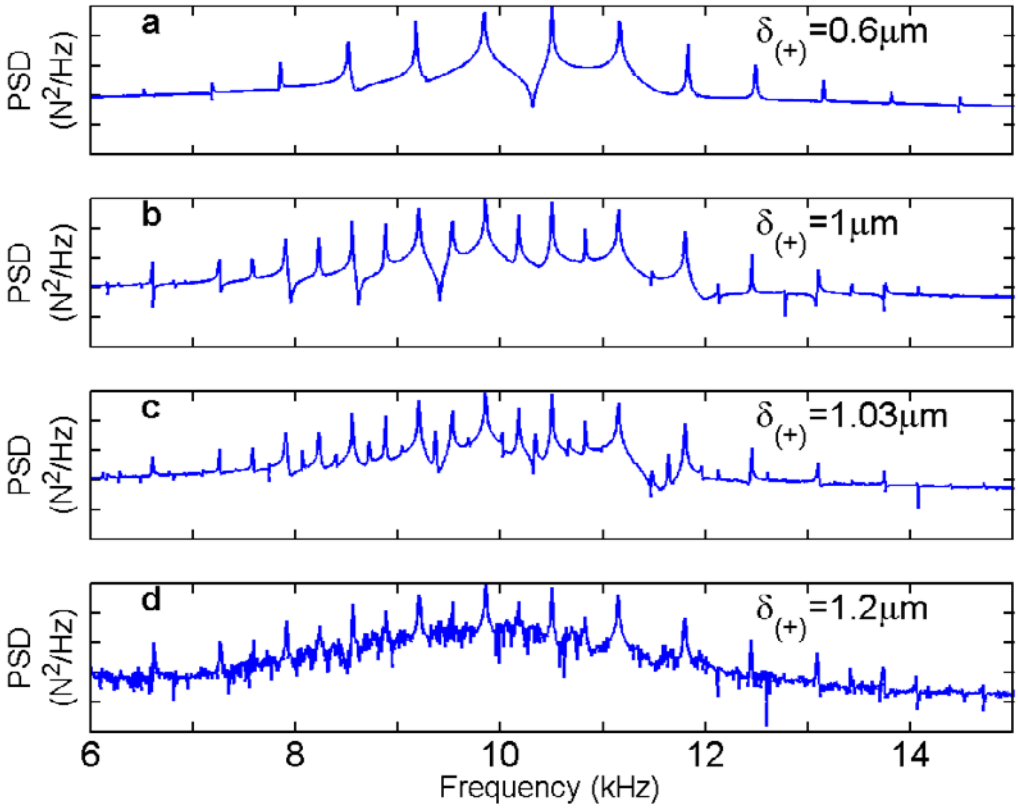

Figure S3. The period doubling cascade route to chaos. PSD of the numerically calculated force-time history, corresponding to driving amplitudes $\delta_{(+)} = 0.6$ μm **(a)**, $\delta_{(+)} = 1$ μm **(b),** $\delta_{(+)} = 1.03$ μm **(c)** and $\delta_{(+)} = 1.2$ μm **(d)** for the fourth particle from the actuator in the forward configuration.

DOI: 10.1038/NMAT3072

Logic. By configuring the tunable frequency mechanical rectifiers to have multiple inputs, we propose tunable frequency logic devices. We present concepts for two types of logic devices: the AND gate (Fig. S4a) and the OR gate (Fig. S4b). We assume incident harmonic signals from A and B are in phase. For the AND gate, a large signal will pass only if the sum of the signals from A and B are greater than the critical amplitude δ_c where the jump phenomenon occurs. Otherwise, if either A or B is off, the signal will be attenuated and not pass. This configuration can also be used in bifurcation-based sensors. For instance, if the signal from A is set near the critical jump phenomena amplitude, a small deviation in B will result in the transmission of a large signal. For the OR gate, a rectifier is placed in each of the A and B branches. If the signal coming from each respective branch is greater than the critical amplitude, this signal will pass and combine with the other signal. Thus a large amplitude signal will pass in all cases except when there is no large signal coming from either A or B.

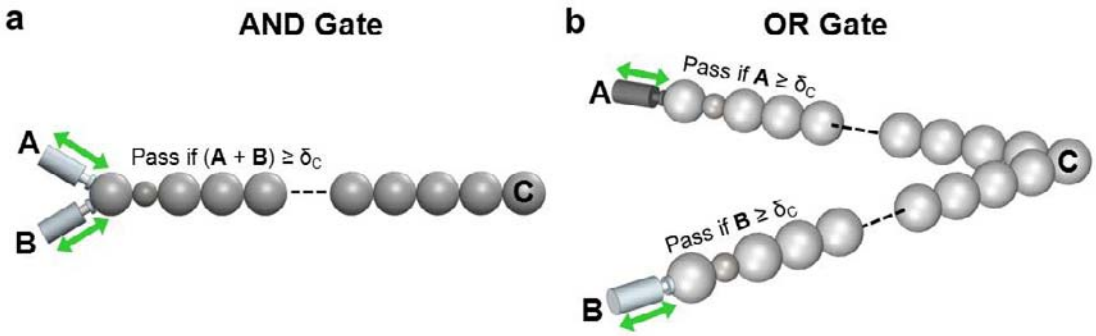

Figure S4. Mechanical logic devices based on the tunable rectifier. Incident signals are applied through A and B, and received in C. **(a)** AND gate. Signals will only pass when combined amplitudes of A and B are greater than the critical rectifier amplitude δ_c. **(b)** OR gate. Signals will pass when either the amplitude of A or B are greater than the critical rectifier amplitude.

System scalability. The proposed system is tunable with changes in static load, and scalable with geometric and material properties. For instance, by reducing the rectifier particle size (see analytical expressions in Methods), assuming $F_0 = 0.1$ N and the same configuration and ratio m/M as in Figs. 1-3, we predict the rectifier has a defect frequency of $f_d \approx 1$ MHz (characteristic of medical ultrasound) and an overall system length of 6.7 mm.

Supplementary Information References

1. Brillouin, L. *Wave Propagation in Periodic Structures.* Dover, New York, NY, (1953).
2. Boechler, N., Theocharis, G., Job, S., Kevrekidis, P. G., Porter, M. A. & Daraio, C. Discrete breathers in one-dimensional diatomic granular crystals. *Phys. Rev. Lett.* **104**, 244302 (2010).
3. Boechler, N., Theocharis, G., Man, Y., Kevrekidis, P. G. & Daraio, C. Defect modes in one-dimensional granular crystals. *arXiv:1103.2483* (2011).
4. Wiggins, S. *Introduction to applied nonlinear dynamical systems and chaos, second edition*. Springer, New York, NY (2000).
5. Ott, E. *Chaos in Dynamical Systems*. Cambridge University Press, Cambridge, UK (1993).